

Some Things About Passive Compensation  
for Space Charge and RF Systems

Eclectic Historical Review

Iowa State Univ., Ames Laboratory ca. 1950 - 55

MURA, Madison Wisc. ca. 1960

Berkely, ca. 1968

Fermilab, ca. 1996

CERN ISR 1975

KEK 1997 - 8

LANL PSR 1998- -01

Fermilab Proton Driver 2000

KEK 2001 JKI Collabor.

400 MeV Capture D\_p/ = +/- .125% [Q=3E13]

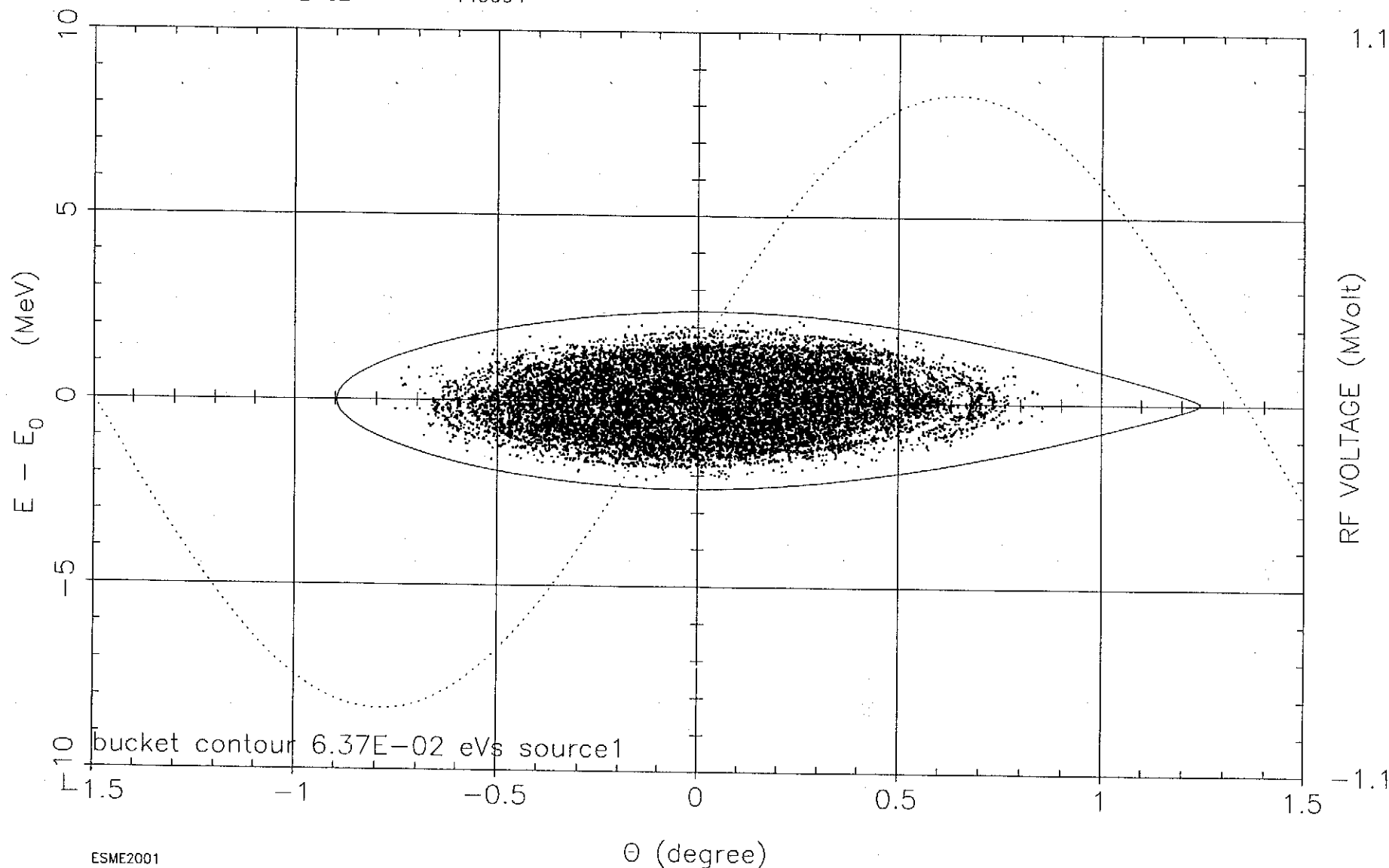
Iter

400

1.323E-03 sec

$H_B$ (MeV)	$S_B$ (eV s)	$E_S$ (MeV)	$h$	$V$ (MV)	$\psi$ (deg)
2.3492E+00	6.3656E-02	1.3673E+03	126	9.301E-01	9.111E+00
$\nu_S$ (turn <sup>-1</sup> )	$\text{pdot}$ (MeV s <sup>-1</sup> )	$\eta$			
1.0964E-01	6.2048E+04	-4.7220E-01			
$\tau$ (s)	$S_b$ (eV s)	$N$			
3.2633E-06	1.4508E-02	149994			

*Space charge plus added inductance included.*

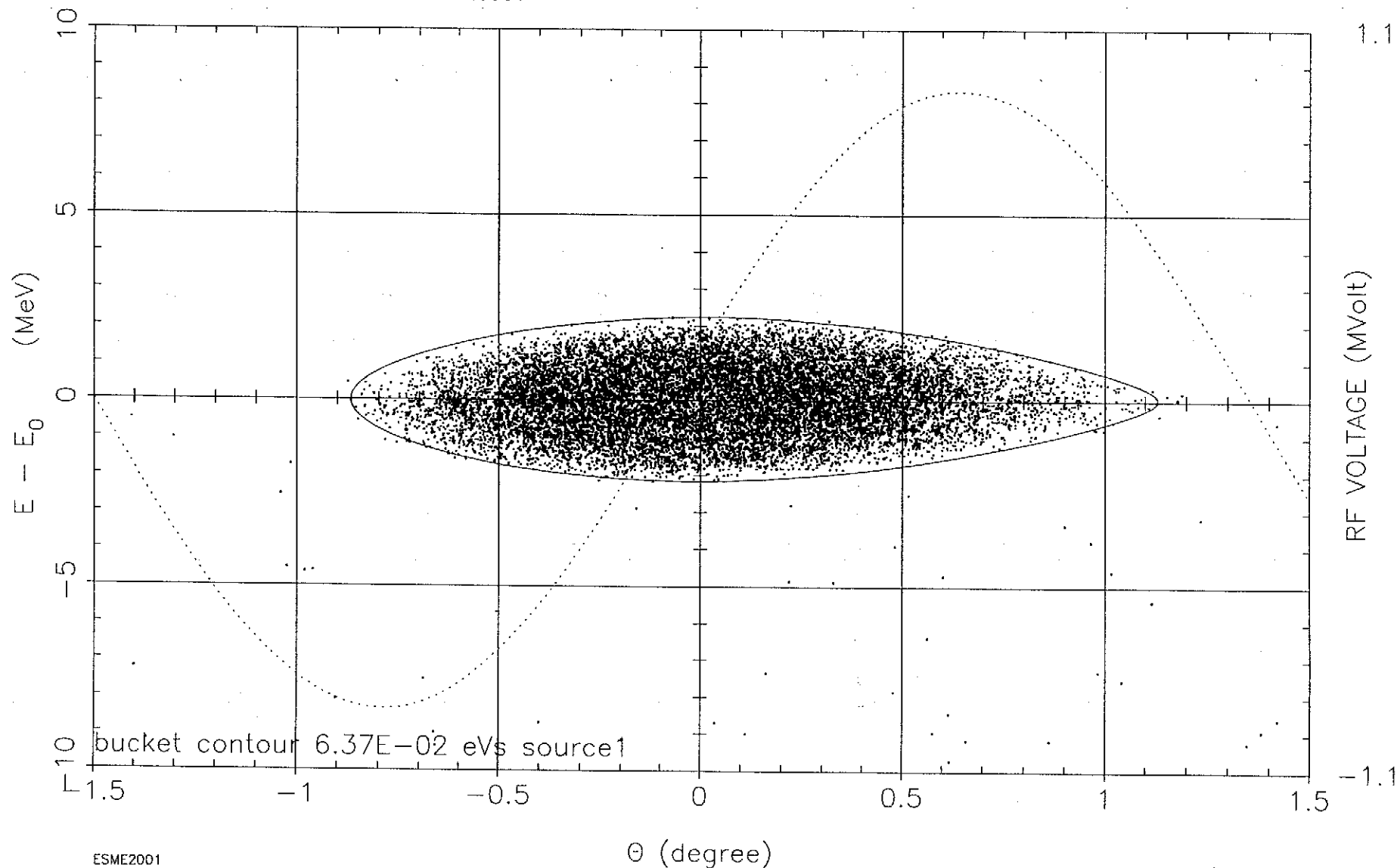


400 MeV Capture D<sub>p</sub>/ = +/- .125% [Q=3E13]

Iter 400 1.323E-03 sec

H <sub>B</sub> (MeV)	S <sub>B</sub> (eV s)	E <sub>S</sub> (MeV)	h	V (MV)	ψ (deg)
2.3492E+00	6.3656E-02	1.3673E+03	126	9.301E-01	9.111E+00
ν <sub>S</sub> (turn <sup>-1</sup> )	pdot (MeV s <sup>-1</sup> )	η			
1.0964E-01	6.2048E+04	-4.7220E-01			
τ (s)	S <sub>b</sub> (eV s)	N			
3.2633E-06	1.9282E-02	149061			

*space charge included in simulation*



400 MeV Capture D<sub>p</sub>

$\epsilon = \pm 0.125\%$   $Q=3E13$

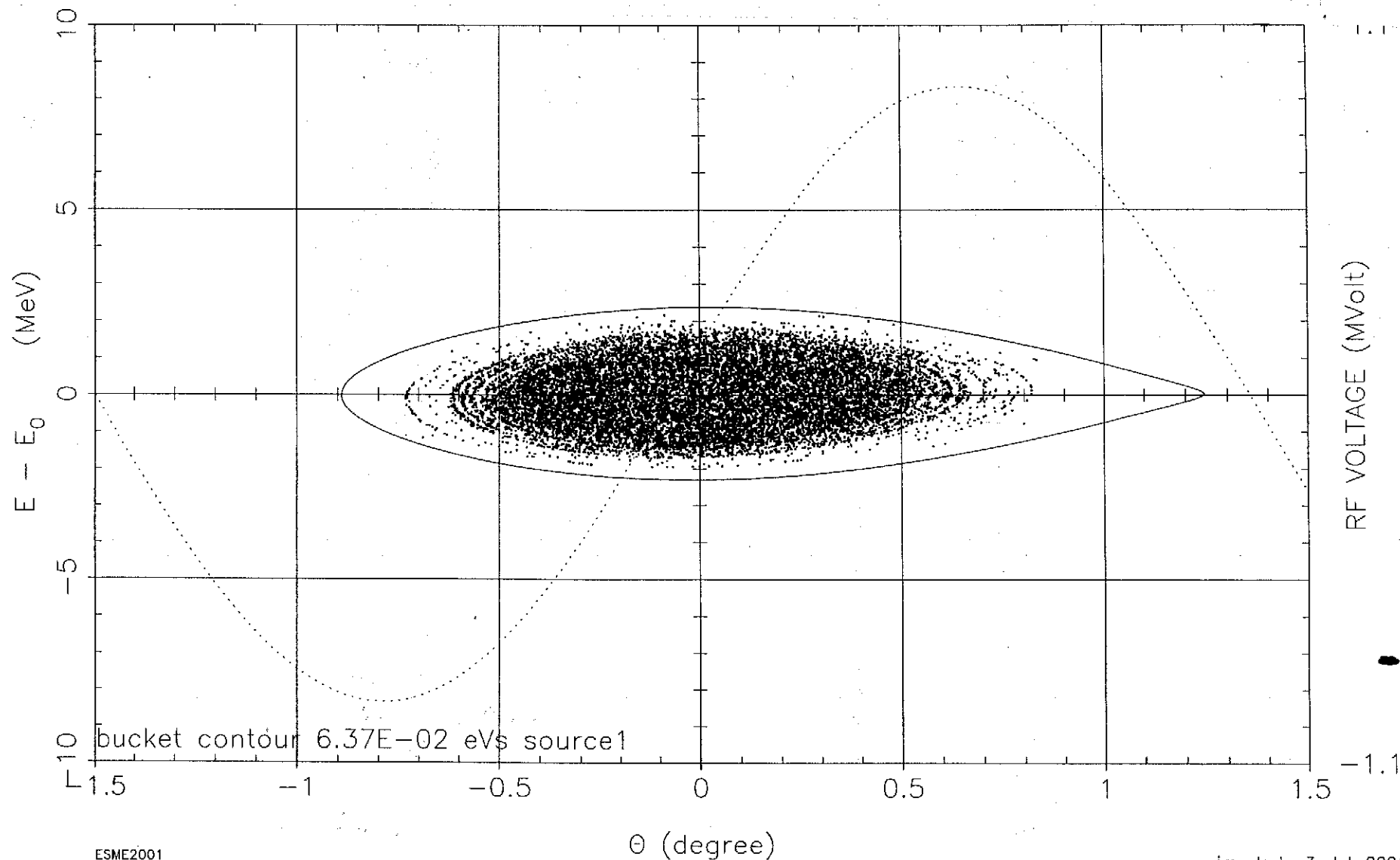
Iter 400

1.323E-03 sec

$H_B$ (MeV)	$S_B$ (eV s)	$E_S$ (MeV)
2.3492E+00	6.3656E-02	1.3673E+03
$\nu_S$ (turn <sup>-1</sup> )	pdot (MeV s <sup>-1</sup> )	$\eta$
1.0964E-01	6.2048E+04	-4.7220E-01
$\tau$ (s)	$S_b$ (eV s)	N
3.2633E-06	1.4107E-02	15000

h	V (MV)	$\psi$ (deg)
126	9.301E-01	9.111E+00

space charge effect  
not included ~~in~~ in simulation



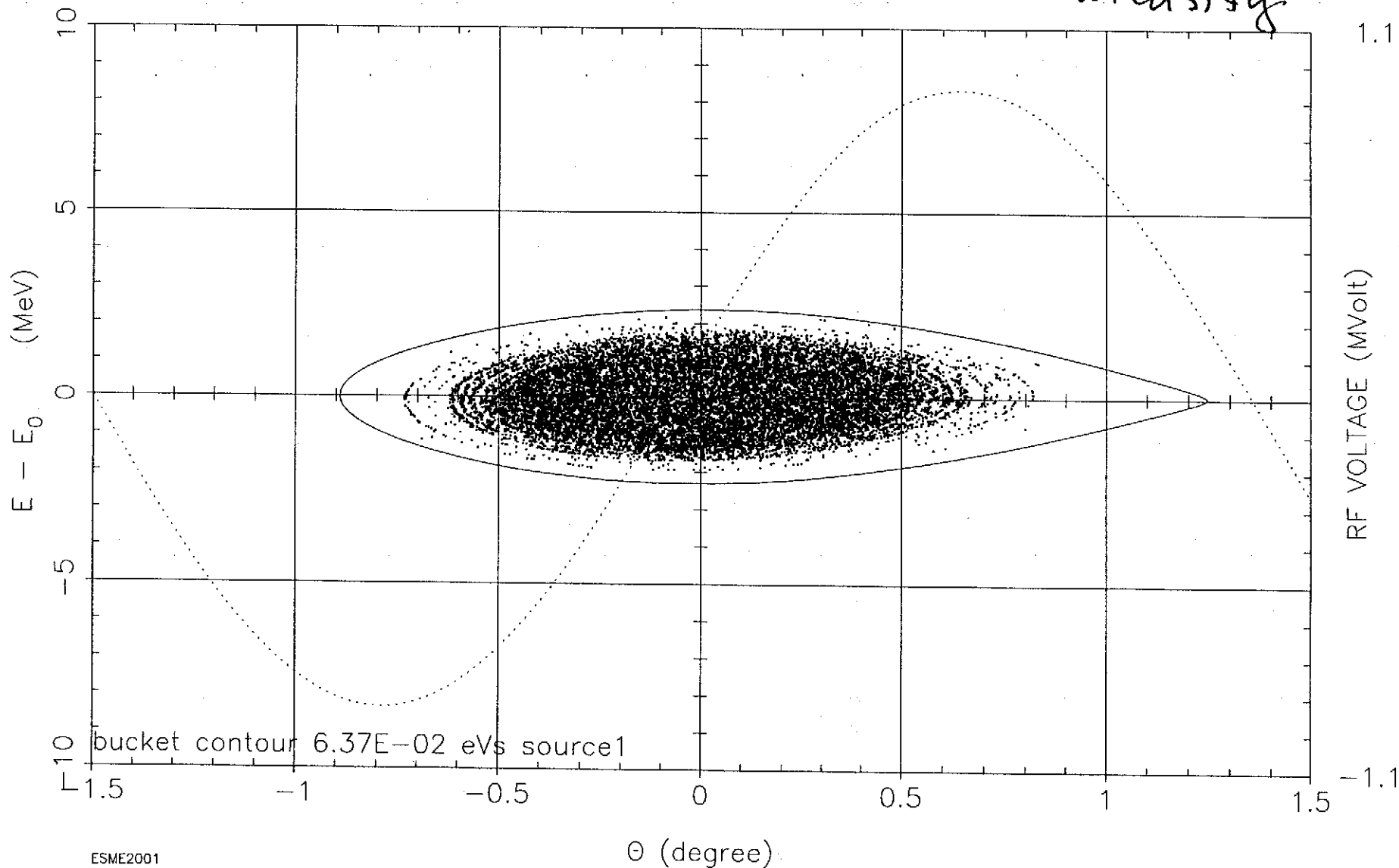
400 MeV Capture D<sub>p</sub>/ = +/- .125% Q=3E13

Iter 400 1.323E-03 sec

H <sub>B</sub> (MeV)	S <sub>B</sub> (eV s)	E <sub>S</sub> (MeV)	h	V (MV)	ψ (deg)
2.3492E+00	6.3656E-02	1.3673E+03	126	9.301E-01	9.111E+00
ν <sub>S</sub> (turn <sup>-1</sup> )	pdot (MeV s <sup>-1</sup> )	η			
1.0964E-01	6.2048E+04	-4.7220E-01			
τ (s)	S <sub>b</sub> (eV s)	N			
3.2633E-06	1.4107E-02	15000			

1.32 m9

Low  
Intensity



400 MeV Capture D<sub>p</sub>/ = +/- .125% Q=3E13

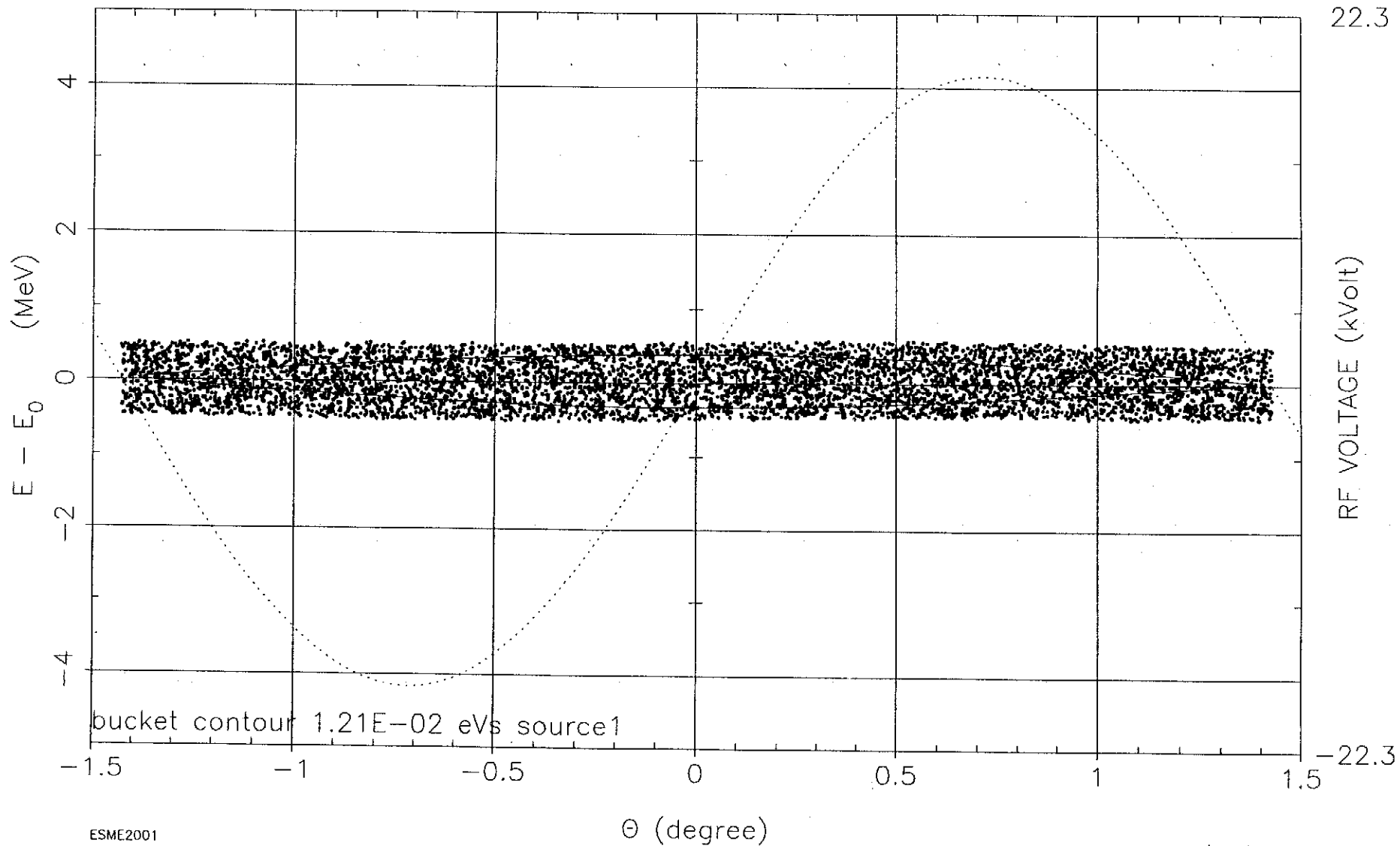
Iter

6

1.997E-05 sec

H <sub>B</sub> (MeV)	S <sub>B</sub> (eV s)	E <sub>S</sub> (MeV)	h	V (MV)	ψ (deg)
3.5970E-01	1.2100E-02	1.3383E+03	126	1.855E-02	0.000E+00
ν <sub>S</sub> (turn <sup>-1</sup> )	p <sub>dot</sub> (MeV s <sup>-1</sup> )	η			
1.6412E-02	0.0000E+00	-4.9284E-01			
τ (s)	S <sub>b</sub> (eV s)	N			
3.3289E-06	1.3709E-02	6000			

*Inj.*



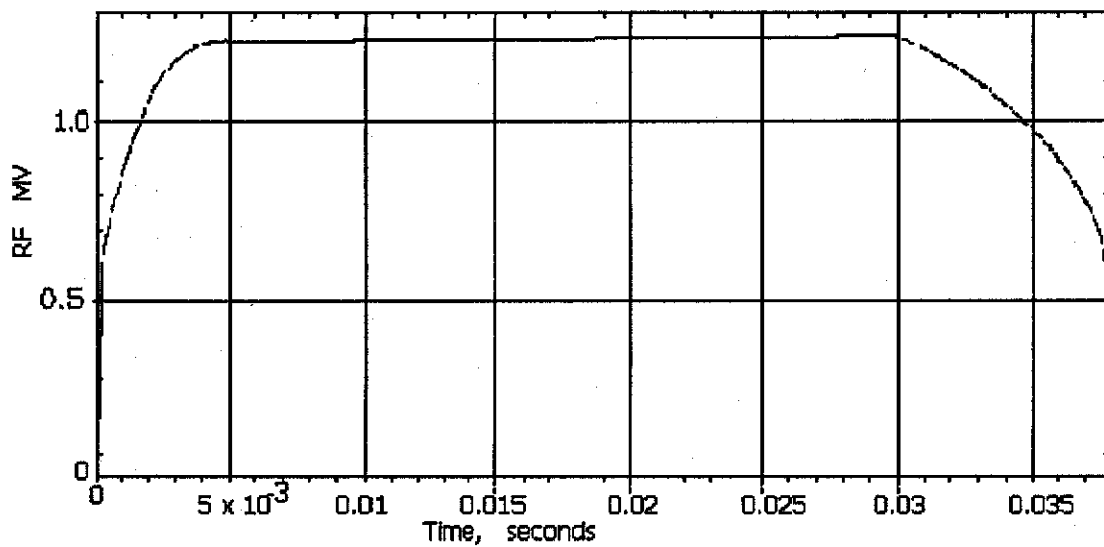


Figure 5.2.1.3, Stage 1 Rf voltage, MV.

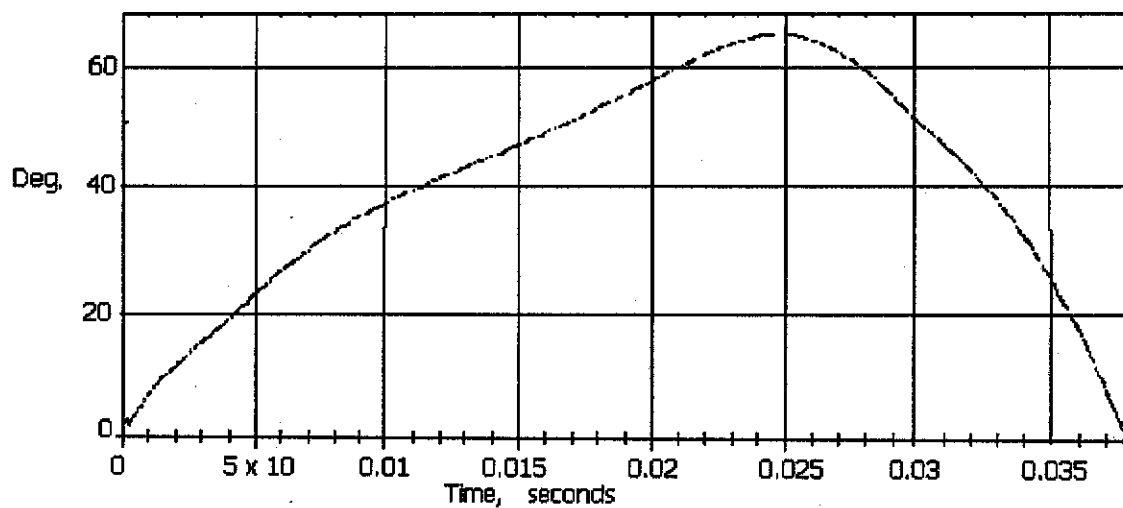


Figure 5.2.1.4 Synchronous phase angle,  $\phi_s$ , during stage 1 acceleration.

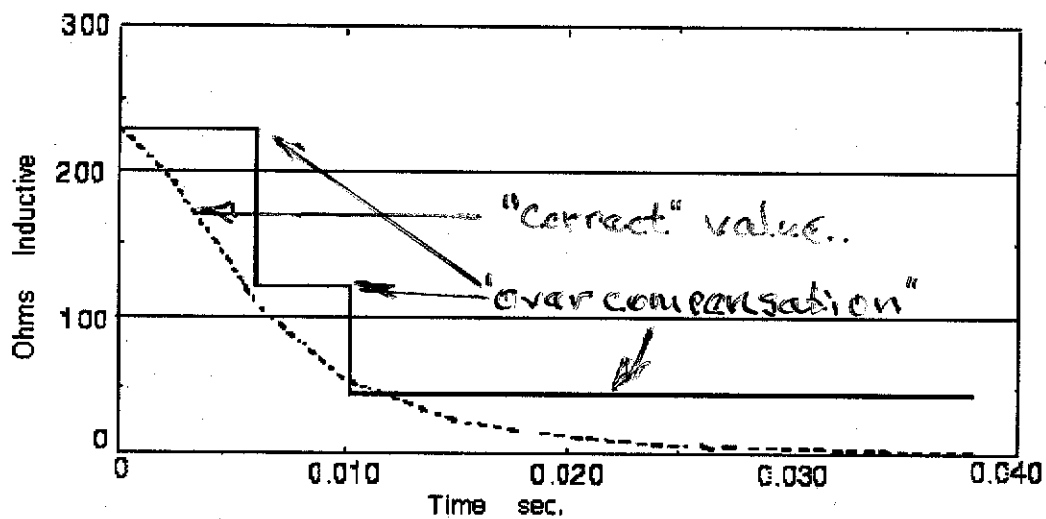


Figure 5.2.1.5 Reactance of the inserted inductor at rotation frequency, ( $h = 1$ ), as a function of time during acceleration.

# Fermi Lab Proton Driver Design. Rpt.

## Capture and Acceleration – Stage 1 Scenario and Modeling

The magnet ramp is driven by a 15 Hz resonant power supply plus an independent second harmonic supply that may be adjusted in phase and amplitude to minimize the required peak rf voltage.

A macro-particle tracking model has been used for the entire cycle from multi-turn injection through matching to Main Injector buckets. The injected protons are assumed to be a continuous coasting beam lasting up to 90  $\mu$ s, timed symmetrically about  $dB/dt=0$ . Other timings have been tried as well, but for an injection period this short nothing better has been found. For nominal linac intensity, 70  $\mu$ s is sufficient to give the required  $3 \times 10^{13}$  protons. The fixed parameters are those from previous table.

The perfectly conducting wall term is the only source of the collective potential included in these simulations.

The rf voltage is raised linearly during injection from 0 to 65 kV. Because of the large slip factor  $\eta$  for this machine, the particles near  $\pm 180$  deg. of rf phase are all captured in this simple maneuver. Certainly some are quite close to the separatrix and subject to later loss because of space charge and limited rf voltage, but these losses are essentially eliminated by use of the inductive insert. They could also be largely eliminated with a substantially higher rf voltage.

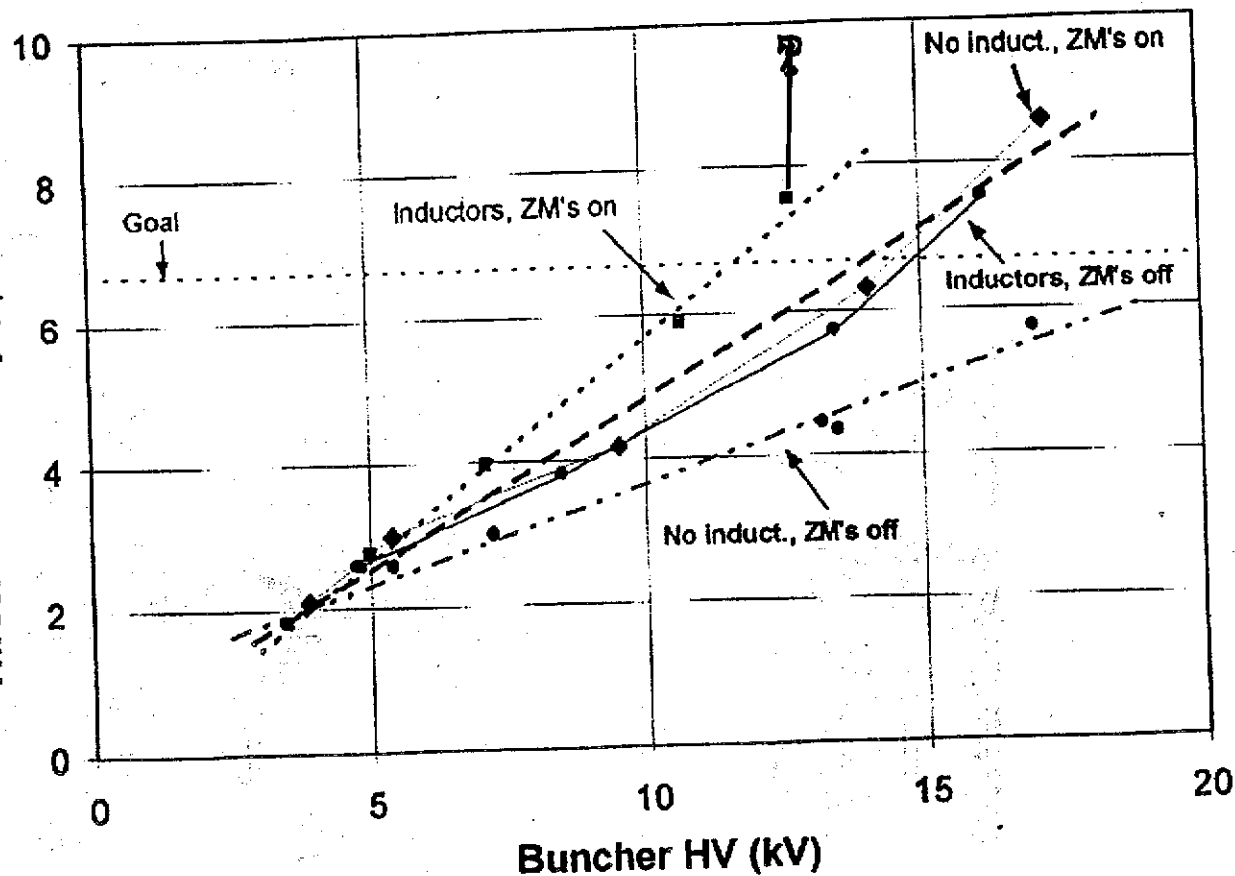
Comparison of RMS emittance at extraction and fractional beam loss during complete cycle for optimum parameters, and for cases each differing from the optimum in a single property.

	Emittance	Beam Loss
Optimum case	0.02 eVs	0.03%
All rf clumped	0.015 eVs	0.21%
rf in two sets	0.018 eVs	0.07%
no inductive insert	0.025 eVs	3.19%

Clearly the inductive insert is a significant element in this scenario; a limited amount of rf focusing is supplemented with self-excited focusing voltage. The character of the inductance curve suggests that there is room for refinement here.



# / 1999 Results from Inductor and Sextupole Tests



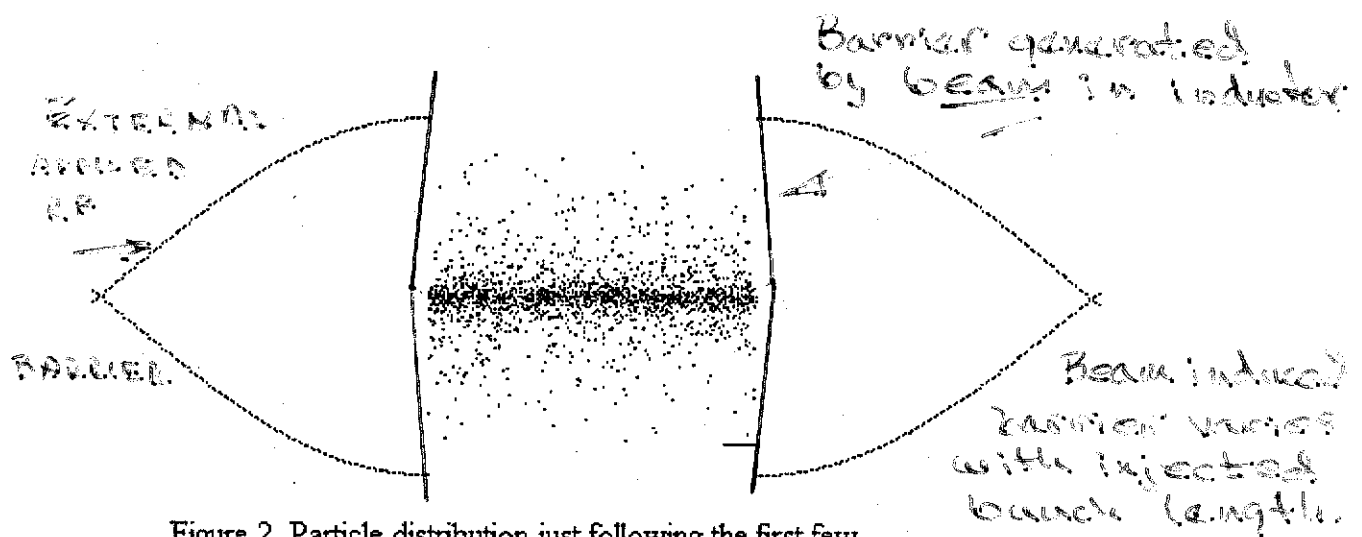


Figure 2. Particle distribution just following the first few turns of injection. The short line is at 3.9 Mev.

Figure 3 shows the distribution after 2800 turns. With no noise or space charge voltages present, the particles remain within the prescribed orbit and the clear gap is maintained.

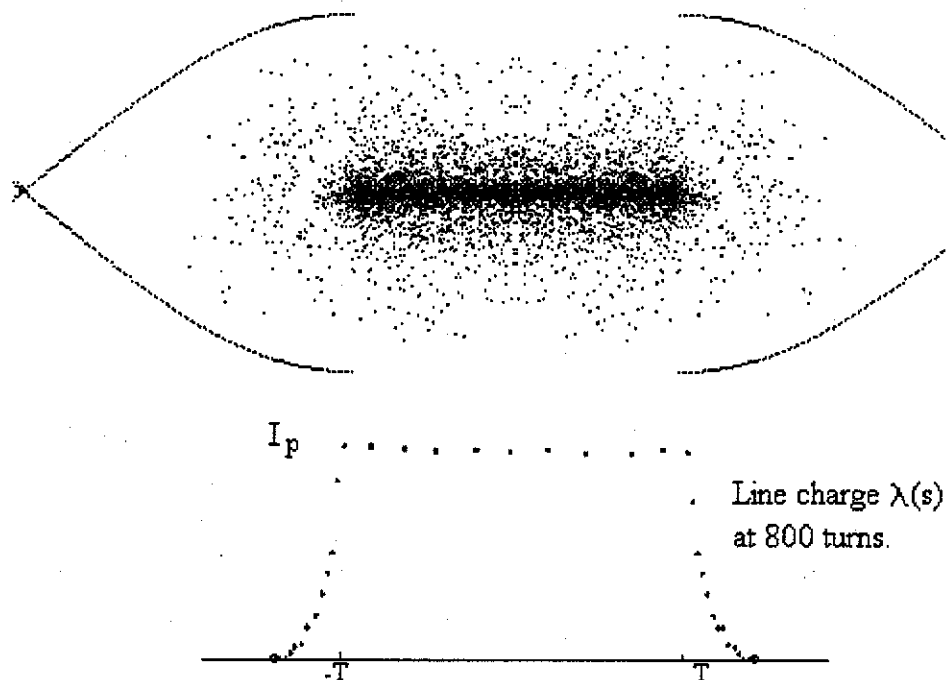


Figure 3. Charge distribution after 2800 turns. The line charge projection  $\lambda(s)$  is for 800 turns.

The projection of space charge density as a function of distance  $s$  along the orbit is shown as  $\lambda(s)$ . Because the high momentum particles move more rapidly around the orbit this function changes as a function of time during filling. This projection represents the distribution at 800 turns. The density appears to decay exponentially at each end of the constant region. These decaying sections

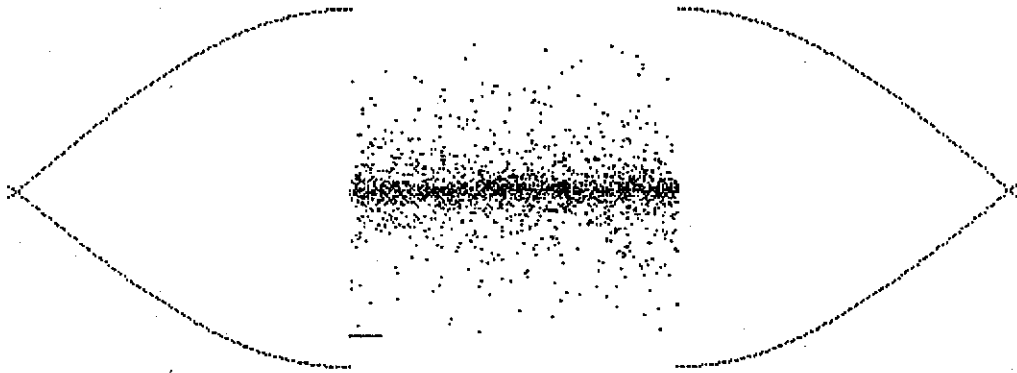


Figure 2. Particle distribution just following the first few turns of injection. The short line is at 3.9 MeV.

Figure 3 shows the distribution after 2800 turns. With no noise or space charge voltages present, the particles remain within the prescribed orbit and the clear gap is maintained.

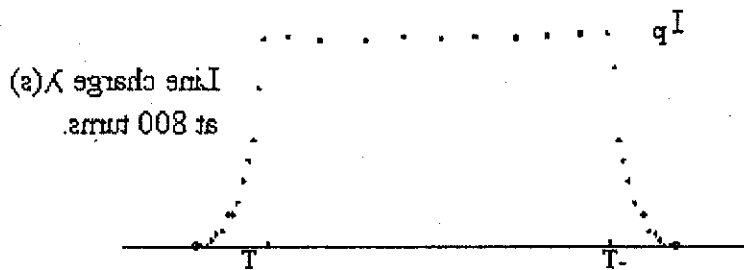
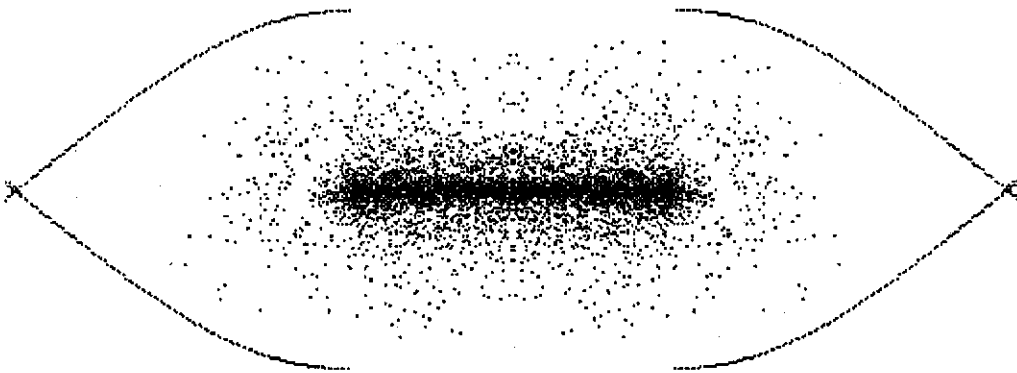


Figure 3. Charge distribution after 2800 turns. The line charge projection  $\lambda(s)$  is for 800 turns.

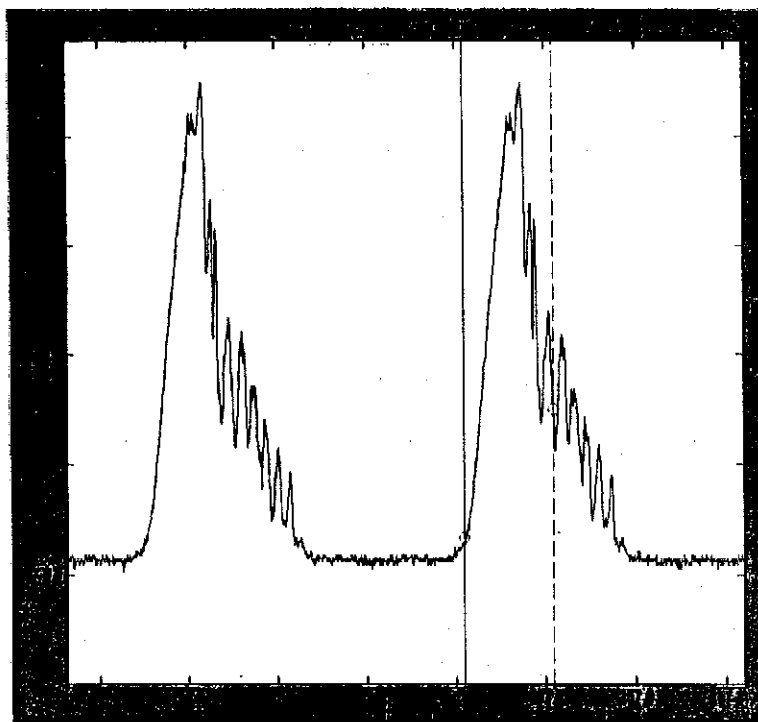
The projection of space charge density as a function of distance  $s$  along the orbit is shown as  $\lambda(s)$ . Because the high momentum particles move more rapidly around the orbit this function changes as a function of time during filling. This projection represents the distribution at 800 turns. The density appears to decay exponentially at each end of the constant region. These decaying sections

# Effect of Heating the Inductor Ferrite

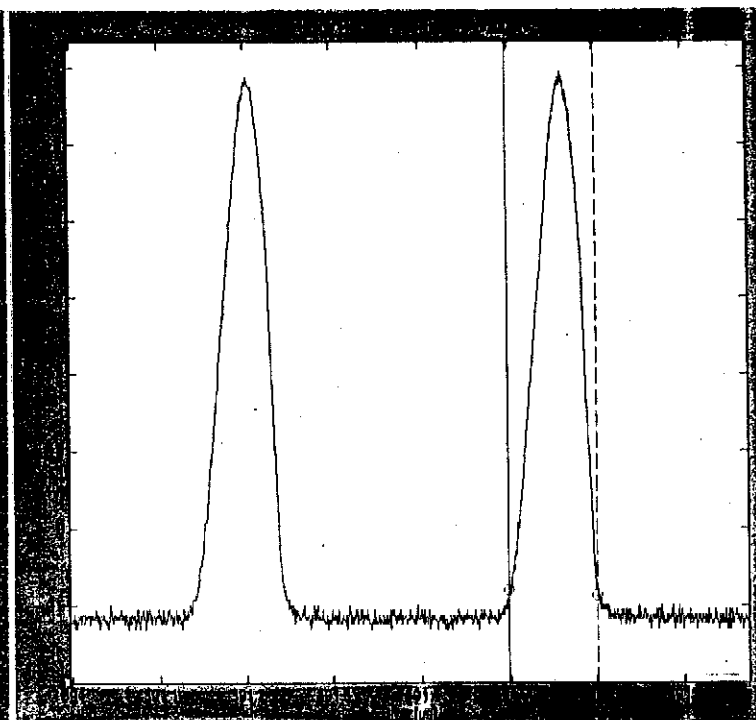
- Ferrite Inductor (2 modules) at room temperature
- 3.3  $\mu\text{C}$  accumulated

- Ferrite at 130° C
- 3.3  $\mu\text{C}$  accumulated
- Longitudinal signal at cavity resonance down 30db from room temperature case

Wall  
Current  
Monitor



Bk91, p150



Bk92, p10

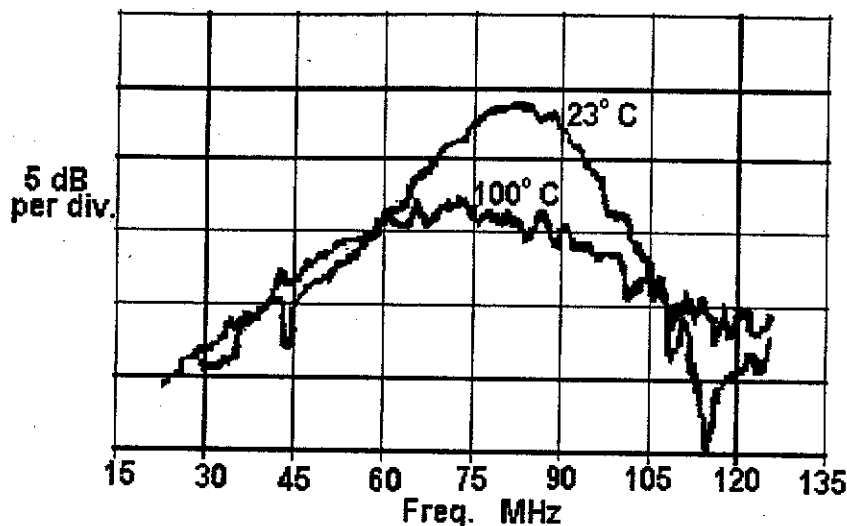


Figure 3. Response curves for resonance measured at 23° C and 100° C. Temperature increase decreases Q and increases magnetic permeability

#### References

- [1] R. Macek and H.A. Thiessen, SPSS Accelerator Enhancement Project, Technical Overview (WBS 1.1.0), (1997).
- [2] D. Neuffer et. al., Particle Accelerators, 23, 133 (1988).
- [3] E. Coulton et.al., Proc. IEEE Particle Accel. Conf. San Francisco, CA, May (1995), p.3134.
- [4] D. Neuffer et.al., Nucl. Inst. and Methods, A 321, 1 (1992).
- [5] S. Hansen et.al., IEEE Trans. Nucl. Sci., NS-22, 1381 (1975).
- [6] A.M. Sessler and V.G. Vaccaro, "Passive Compensation of Long. Space Charge Effects in Circular Accelerators", CERN 68-1, ISR Div. (1968).
- [7] R.K. Cooper, D.W. Hudgings, and G.P. Lawrence, LANL PSR Tech. Note 100, (1982, unpublished).
- [8] T. Hardek, LANL PSR Tech. Note 102, (1982, unpublished).
- [9] A. Hofmann, "Single Beam Collective Phenomena - Longitudinal", CERN 77-13, (1977) 139.
- [10] K. Koba et.al., "Long. Impedance Tuner using High Permeability Material", JHF Ring Memo 309, KEK Jp. (1997)
- [11] M. Plum et.al., "Experimental Study of Passive Compensation of Space Charge at the LANL Proton Storage Ring" Physical Review Special Topics - Accelerators and Beams, Vol.2, 064201 (1999).
- [12] J.E. Griffin, "Radial Transmission Line Treatment of Spurious Resonance in Ferrite Cylinder Space Charge Compensation System" Fermilab, (2001, unpublished).
- [13] K.Y. Ng.....

Note. - Resonant frequency lower at higher temperature.

Both  $\mu'$  and  $\mu''$  increase.

This results in overcompensation by 30 - 50 % depending on temperature.

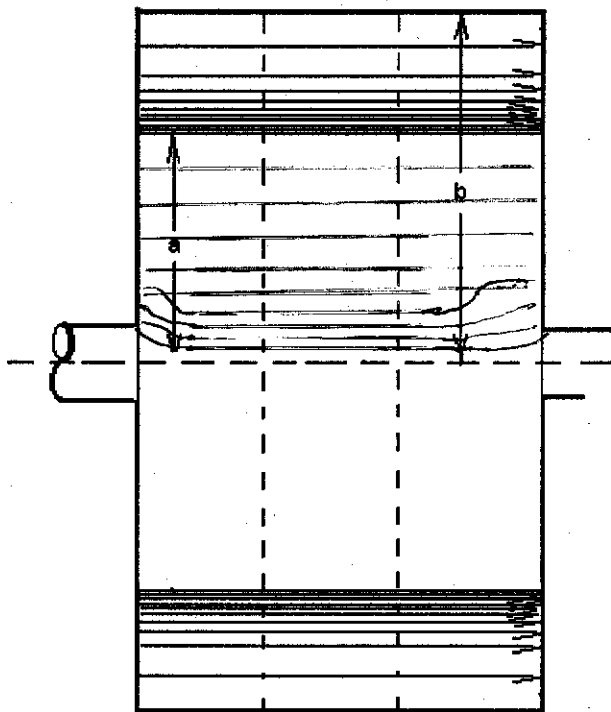
# **The Determination of Resonant Modes in Inductive Inserts for Use in the FNAL Booster**

**Daniel Garcia**  
**Fermi National Accelerator Laboratory**  
**&**  
**Massachusetts Institute of Technology**  
**May 24 – August 10**

## **Abstract**

In response to the apparent success of inductive inserts installed at Los Alamos's Proton Storage Ring, two new inserts have been built to compensate for the effects of longitudinal space charge in the Booster at FNAL. These cavities contain resonant modes that could be excited by the Booster's beam. Thus, the cavities were experimentally examined to distinguish which frequencies would be at risk for causing self-bunching of the beam or coupled bunch oscillations.

## FERRITE RADIAL TRANSMISSION LINE



First consider only E and H fields within the ferrite.

Ignore  $R$  loss in metal shell. Consider only power loss in ferrite due to  $\mu''$ .

$$E_z = A H_0^{(1)}(kr) + B H_0^{(2)}(kr)$$

$$H_\phi = \frac{i}{\eta} \{ A H_1^{(1)}(kr) + B H_1^{(2)}(kr) \}$$

Set  $E_z = 0$  at  $r = b$ .

Set  $H_\phi = 0$  at  $r = 0$

Later consider the effect of additional stored electrical energy within the region from the ferrite to the axis, using 'periodic' boundary conditions between the dashed lines.

At resonance the total stored energy equals  $2 \times \overline{W}_H$ .

Because the same integral expressions are used to develop  $W$  and  $P$ ,  $Q = \frac{\mu'}{\mu''}$

The E and H integrals, sans constants, are;

$$\int_{0.0635}^{0.1} \left[ \left( \cos(\theta_0) \cdot Y_1(kr) - \left( \sin(\theta_0) \cdot J_1(kr) \right) \right) \right] \left[ \left( \cos(\theta_0) \cdot Y_1(kr) - \left( \sin(\theta_0) \cdot J_1(kr) \right) \right) \right]^* r dr$$

$$\int_{0.0635}^{0.1} \left[ \left( \sin(\theta_0) \cdot J_0(kr) - \left( \cos(\theta_0) \cdot Y_0(kr) \right) \right) \right] \left[ \left( \sin(\theta_0) \cdot J_0(kr) - \left( \cos(\theta_0) \cdot Y_0(kr) \right) \right) \right]^* r dr$$

$$\overline{W}_H = \frac{\mu'}{4} \int HH^* dV \quad P = \frac{\omega \mu'}{2} \int HH^* dV$$

By setting the resonant frequency to 76 MHz and balancing the electrical and magnetic energy by varying,  $\mu'$  one finds values for  $k$  and  $\mu'$ .

Now, using measured  $Q = 3.5$ , one finds  $\mu'' = 12.9$ .

Using this value for  $\mu''$  in the above power expression one can find a value for  $R_{sh}$

The result is that  $R_{sh}$  is almost exactly 9 kOhms per meter.

# RADIAL TRANSMISSION LINE TREATMENT OF SPURIOUS RESONANCE IN FERRITE CYLINDER SPACE CHARGE COMPENSATION SYSTEM

James E. Griffin

## Introduction

Several meters of ferrite rings (Toshiba M4C21A) tightly packed within  $\sim 1$  m stainless steel tubes, have been installed in the Los Alamos Nat'l. Lab. Proton Storage Ring (PSR) for the purpose of cancellation of longitudinal space charge effects [1,2]. After the installation, high intensity operation of the ring was hampered by a serious spontaneous self-bunching (SSB) instability at rotation harmonic 26 (72.67 MHz.). Two turns of the PSR beam current, with well developed instability bunching, as detected by a broad-band longitudinal pick-up, are shown in Figure 1.

At Fermilab a seven core section of a similar ferrite inductor was assembled and excited at each end by small antennae. In this experiment there was no longitudinal conductor extending along the axis, so longitudinal electric fields were not 'shorted out' or attenuated by a parallel inductance. Signals developed in the ferrite by network analyzer excitation were observed at high sensitivity at the 'output' antenna. A relatively narrow resonance with center frequency near 84 MHz was observed. The 3 dB bandwidth of the resonance appears to be  $\sim 21$  MHz, resulting in  $Q \sim 3.9$ . The observed resonance is shown in Figure 2. It is the purpose of this note to examine the hypothesis that a resonance such as this may be characterized as a standing wave  $TM_{010}$  radial transmission line resonance of the ferrite cylinder coupled to the vacuum space within the cylinder.

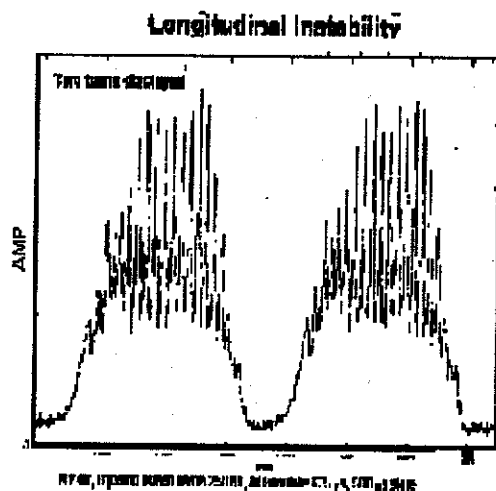


Figure 1. Two turns of LANL injected beam with well developed instability

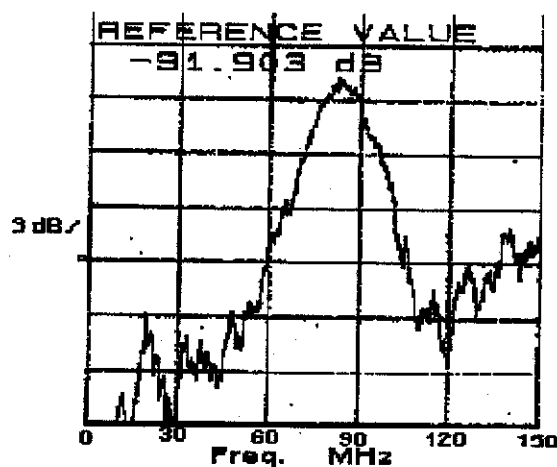


Figure 2. Resonance observed in model of ferrite cylinder space charge correcting insertion. LANL PSR



First results from LANL were encouraging but equivocal. Ferrite removed.

About one year later, when upgrade results were not quite as good as anticipated, ferrite tanks were reinstalled. Results were promising, but a self-bunching ( $\mu$ -wave-like) instability at high intensity was observed.

Again ferrite tanks removed. Could we design some ferrite inductors that would not generate instability.

Last year Dave Wildman, Milorad Popovic, and I assembled a stack of cores to investigate the problem. We located a  $TM_{01}$  (??) resonance near the offending frequency  $\sim 77$  MHz. Resonance Q appears to be about 2, not inconsistent with available data on the ferrite.

I wanted to change the ferrite permeability selectively along the tank to spread the resonance. This was to be done by attaching permanent magnets to the outside. After a few broken fingers and inconclusive data we decided this was not going to work.

Milorad said "heat the ferrite, that will reduce the Q, and maybe also increase the permeability!" Score at least one for Milorad.

At latest hearing the tanks are reinstalled in the PSR with heating blankets. Results no longer equivocal.

There is at least one moral.

With stationary rf bucket, bunch length =  $\text{Const.} \times (V_{rf})^{1/4}$

Rf power is expensive to buy and operate. Certainly more than ferrite.

Let the beam do the work.

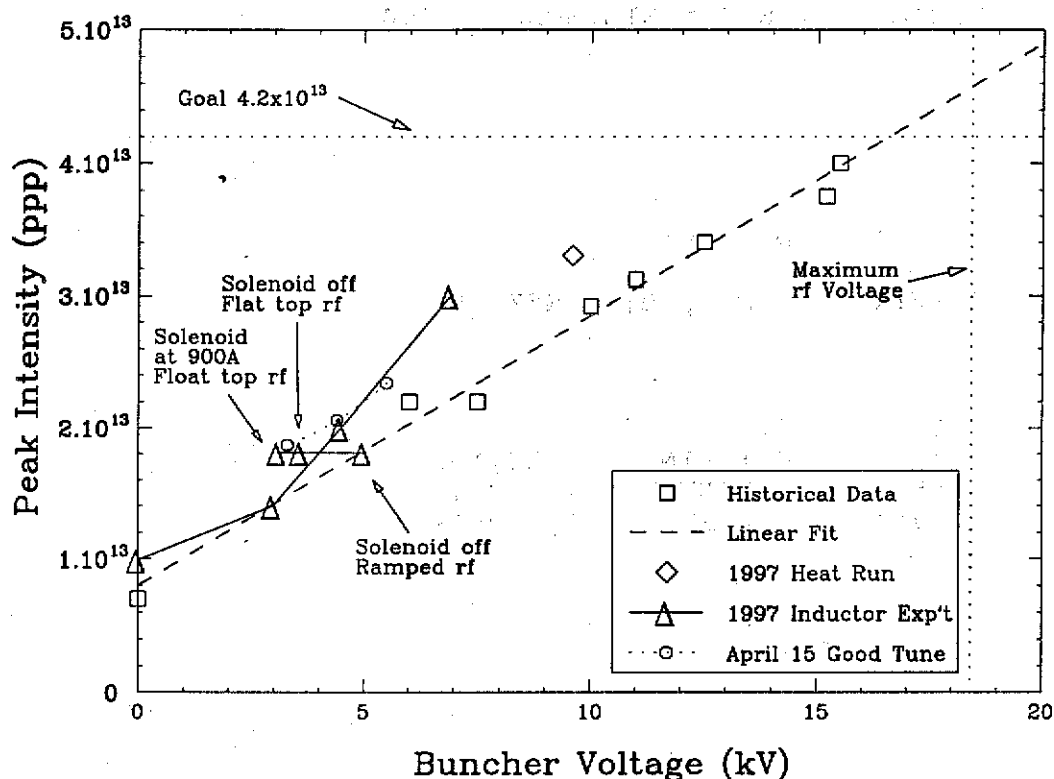


FIG. 5. Stability threshold versus rf voltage improvement. Results of this experiment are depicted by triangles.

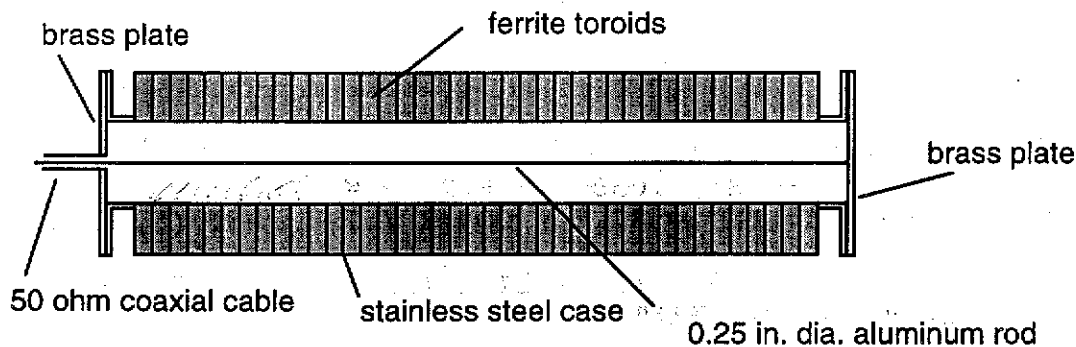


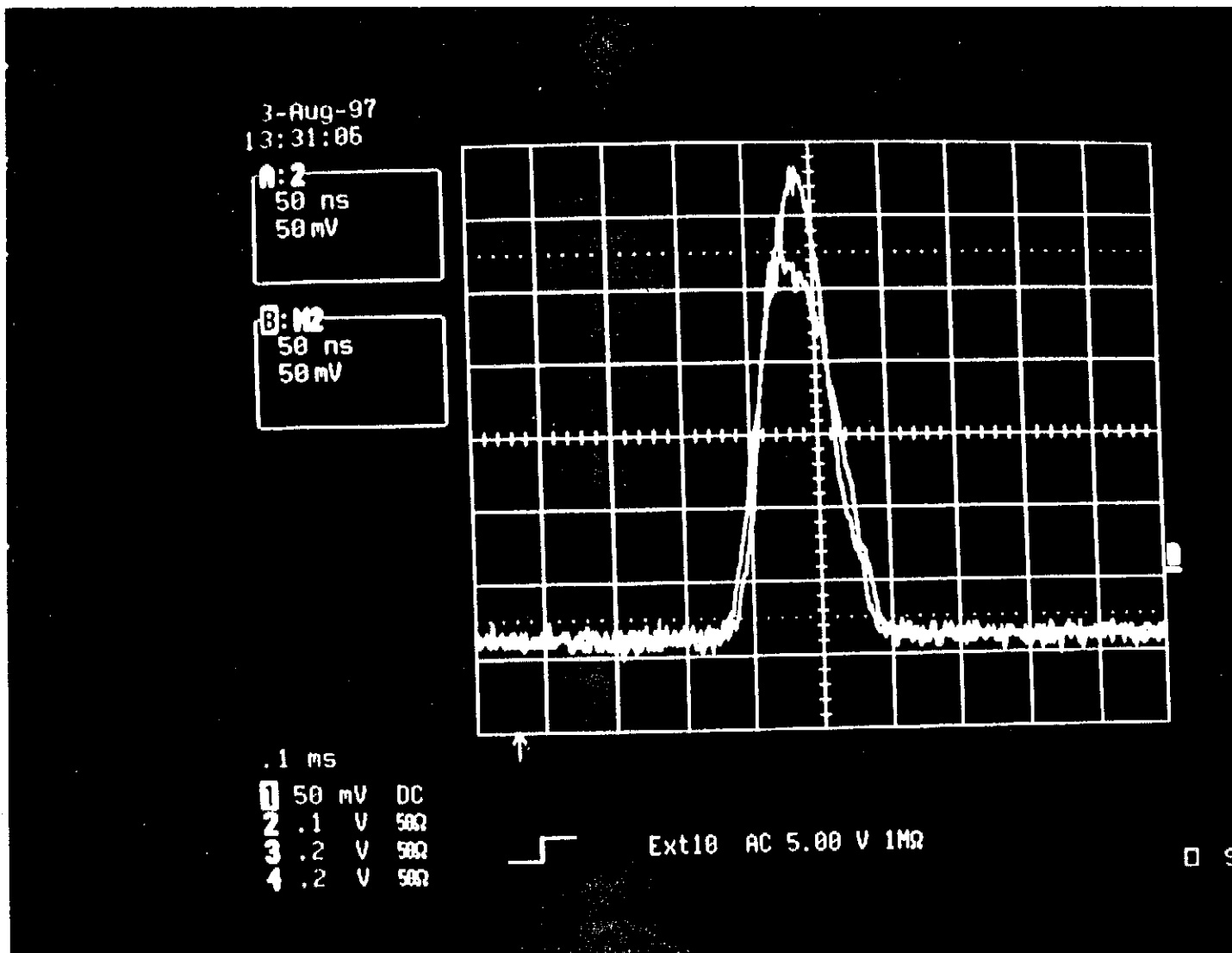
FIG. 6. Schematic cross section of the measurement setup with test fixtures.

• Inner surface of each ring coated (baked on) with thin conductive coating. ~ 1000  $\Omega/\text{sq}$ .

Hearings (???)

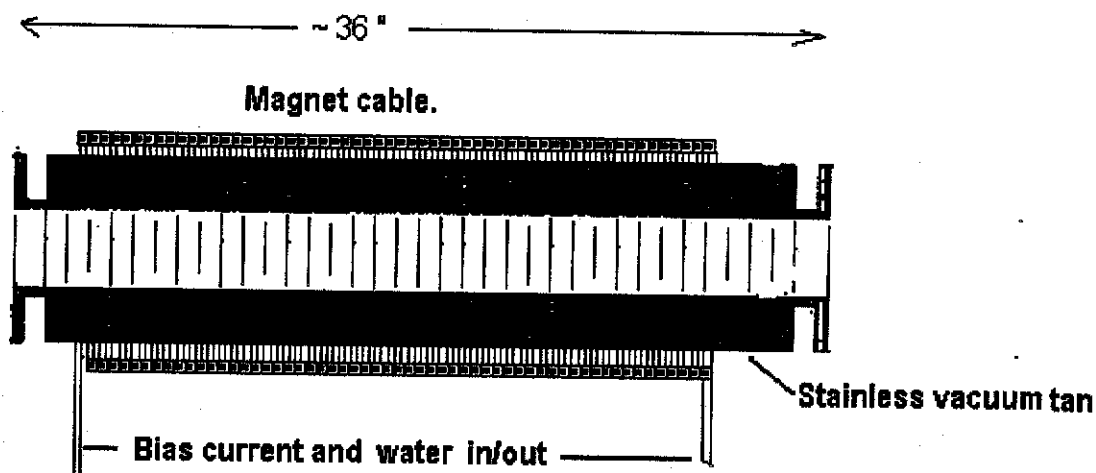
Also each core had small radial conducting Pads baked on.

8/3/97



Lower Trace solenoid on 900A 625μs

# LANL Inductor Injection Experiment



Ferrite inductor module. 8" o.d. 5" i.d. cores in s.s. tank with vacuum flanges. Water temp. varia

Inductance at low bias  $\sim 4.5$  Hy/m. At 632 kHz, (injection) inductive reactance  $\sim 18$  Ohms / m.

As  $\beta\gamma^2$  increases, required inductance decreases. As  $\beta$  increases, inductive reactance for,  
given inductance increases. So bias during acceleration almost certainly necessary.

The inner surface of each core was coated with a baked on conducting surface, about  $1000 \Omega/\text{sq}$ . Also each core had a narrow radial path from the inner surface to the outer container baked on.

# LONGITUDINAL IMPEDANCE TUNER USING HIGH PERMEABILITY MATERIAL

K.Koba, D.Arakawa, M.Fujieda, K.Ikegami, C.Kubota, S.Machida, Y.Mori, C.Ohmori, K.Shinto, S.Shibuya, A.Takagi, T.Toyama, T.Uesugi, T.Watanabe, M.Yamamoto, M.Yoshii  
KEK, 1-1 Oho, Tsukuba-shi, Ibaraki-ken, 305, Japan

## Abstract

Space charge effects cause the emittance growth and the beam instability, when the short bunched beams are accelerated in a high intensity proton synchrotron. The impedance tuner using high permeability materials has been developed to cancel the longitudinal space charge effects.

We installed the impedance tuner in the main ring of KEK proton synchrotron (PS) and observed the canceling effect.

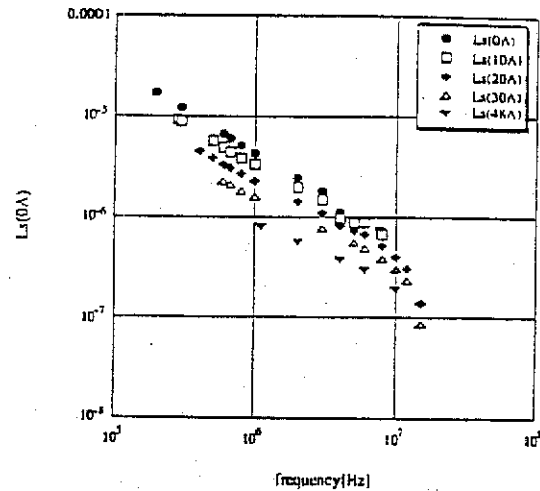


Fig1. The inductance as a function of frequency is measured with a bias current from 0 to 48A/turn.

## 3. Experimental setup

The impedance tuner consists of eight cores of FINEMET with 6 turn bias coil as shown in Fig.2. The bias coil has "8" shape to eliminate the beam induced RF currents. All the cores are installed in a cylindrical vacuum chamber. The bias current is varied from 0 to 30 A (0 to 180 A · Turn).

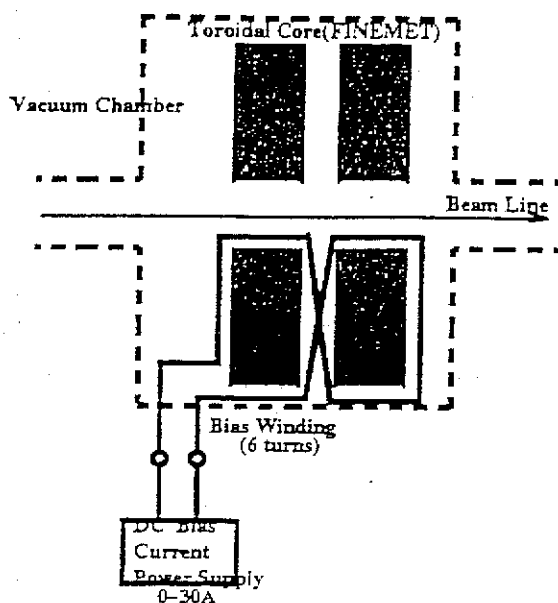


Fig.2 Experimental setup of the impedance tuner installed in the KEK PS main ring

## 5. Results

The frequency shift as a function of intensity is plotted in Fig.5. The dashed line is a fitted line of a data before installation and the solid line is that after the installation. The slope of dashed line can be solely explained by space charge impedance, that is calculated as 440 ohms. On the other hand, the slope of solid lines is halved. Therefore, the inductive impedance made by the FINEMET cancels the half of the space charge impedance.

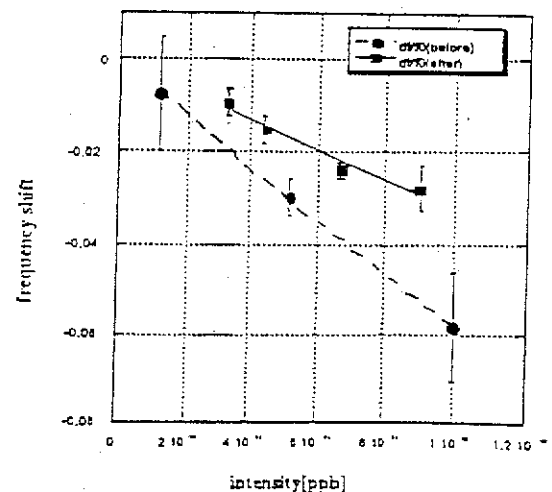


Fig.5 The measured frequency shifts of the quadrupole oscillations as a function of the beam intensity are plotted.

## INDUCTIVE CAVITIES FOR PSR LONG BUNCH MODE

R. K. Cooper, D. W. Hudgings, and G. P. Lawrence

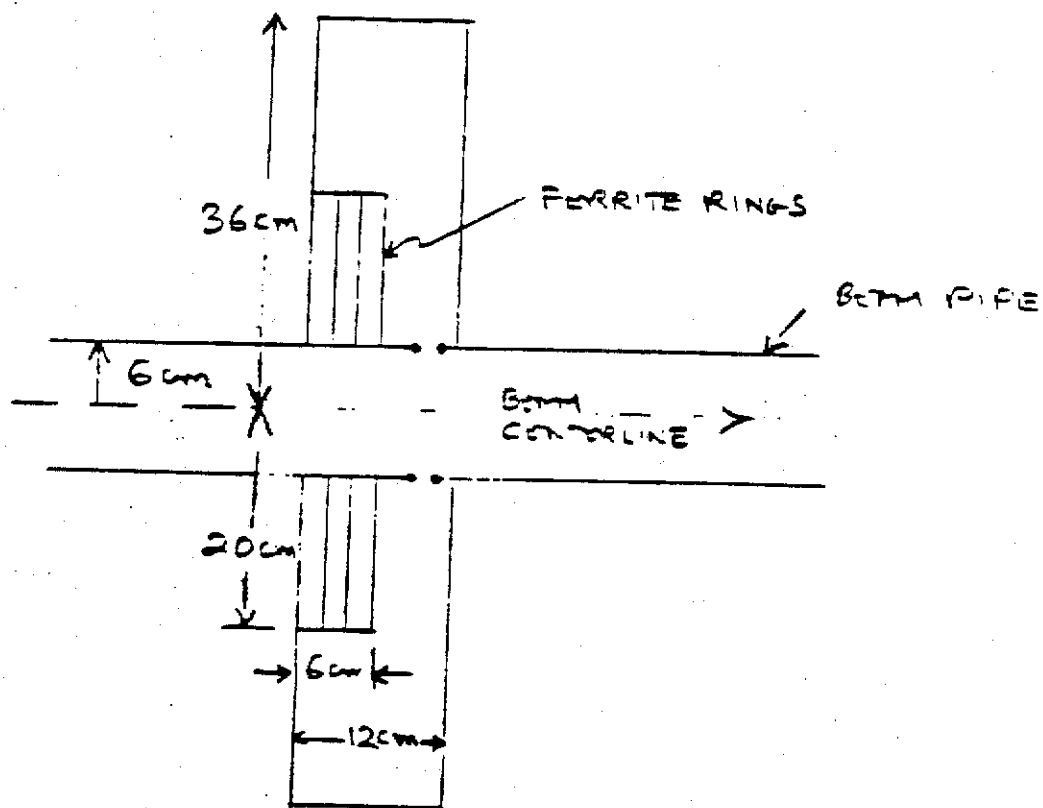


Fig. 5. Possible design for unit of a 20 element distributed inductive insert system (approximately to scale).

## Inductive Insert Passive Space Charge Studies

In 1996 or 1997, in the early phase of the Fermilab Proton Driver and/or muon collider design, I proposed a study of the passive space charge compensation idea to combat space charge interference with short bunch preparation by bunch rotation.

At the same time K. Koba and collaborators at KEK Laboratory in Japan initiated an experiment in the 12 GeV Proton Synchrotron.

In 1982 an inductive insert was proposed for the LANL PSR by R. Cooper, D. Hudgings, and G. Lawrence. (Also another by T. Hardek I think.) No results are reported.

In 1997, in order to test the concept in the best possible machine, D. Wildman and I built two ~ 1 m. ferrite inductor tanks at Fermilab, using old, discarded (but carefully preserved) Toshiba M4C21<sub>a</sub> ferrite. We persuaded B. Macek to allow installation for a two day test prior to upgrade shutdown in August 1997. Results were equivocal but encouraging. The inserts were removed following the first studies.

After the upgrade shutdown the tanks were re-installed, with promising results. But self-bunching instability at high intensity forced removal. The cause of the instability (also somewhat equivocal) was determined to be a tank/ferrite resonance near 80 MHz.

As a result of an ingenious suggestion by M. Popocic (Fermilab), the Q and shunt impedance of the resonance were reduced to a safe level by heating the ferrite. The tanks were reinstalled with controlled heating and are operating successfully. The PSR has reached record intensity using skew quadrupoles, Landau damping, and ferrite.

LANL  
PSR

ORGANISATION EUROPÉENNE POUR LA RECHERCHE NUCLEAIRE  
**CERN** EUROPEAN ORGANIZATION FOR NUCLEAR RESEARCH

PASSIVE COMPENSATION OF LONGITUDINAL SPACE CHARGE EFFECTS

IN CIRCULAR ACCELERATORS: THE HELICAL INSERT

A. M. Sessler \*  
CERN, Geneva, Switzerland

and

V. G. Vaccaro  
CERN, Geneva, Switzerland

G E N E V A

1968

---

\* On leave of absence from the Lawrence Radiation Laboratory,  
University of California, Berkeley, California.



## STABILIZATION OF INTENSE COASTING BEAMS IN PARTICLE ACCELERATORS BY MEANS OF INDUCTIVE WALLS†

R. J. BRIGGS and V. K. NEIL

Lawrence Radiation Laboratory, University of California, Livermore, California

(Received 8 November 1965)

878<sub>2</sub>

A method for stabilizing a relativistic coasting beam against the negative mass instability is described. It is shown that a beam above the transition energy can be stabilized, even in the case of a frequency spread in the beam, by making the wave impedance at the beam inductive. Several possible structures that can result in such an inductive impedance are described, and the case of a dielectric material positioned against the tank wall is analysed in detail. The effect of the dielectric wall on the longitudinal and transverse resistive instabilities is considered. It is shown that a dielectric can also play an important role in the stability criteria for these resistive modes, and in some cases can make the requirements on the frequency spread for stability less stringent. Several numerical examples are given to illustrate the typical range of the parameters involved.

### 1. INTRODUCTION

A relativistic beam of charged particles circulating in an accelerator can be unstable to the 'negative mass' instability (NIELSEN *et al.*, 1959). The form of the perturbation is a longitudinal (azimuthal) density modulation of the beam, and the coupling mechanism is the longitudinal electric field arising from the perturbation. A usual physical explanation of the instability is that the particles at the front of a bunch of increased density feel a longitudinal force in the forward direction. If the particle energy and the form of the magnetic guide field is such that the circulation frequency of the particles is a decreasing function of energy (above the transition energy), this results in an increase in orbiting radius and a decrease in azimuthal velocity. Particles at the back of the bunch move backward towards the region of increased density. Similarly, particles at the back of the bunch feel a deceleration and move forward toward the region of increased density. Particles behave, as far as azimuthal motion is concerned, as if they had a negative mass. Radial electromagnetic forces arising from the perturbation can also have an effect on the instability (NEIL and HACKROTTE, 1965), but this is a negligible effect in most particle accelerators.

This instability may be overcome by a sufficient spread in particle circulation frequency and/or transverse oscillation amplitudes (NIELSEN *et al.*; NEIL, 1963). In this work we shall investigate a stabilization method that does not rely on such mechanisms. The method is suggested by an analogy between the circulating beam and a beam in rectilinear motion, such as those used in many microwave beam tubes. A beam in rectilinear motion is a 'positive mass' beam in the sense of the preceding paragraph. If the beam is surrounded by perfectly conducting walls, a longitudinal density modulation impressed on the beam will not grow, but will undergo stable oscillations. The behaviour of these stable space-charge waves is radically altered if the conducting walls are replaced by a wall with an impedance  $Z = R + iX$ , where  $Z$  is the impedance of the wall and  $R$  and  $X$  are real quantities. For a transverse magnetic wave (*E*-wave)

† Work performed under the auspices of the U.S. Atomic Energy Commission.

888

# STABILIZATION OF NON-RELATIVISTIC BEAMS BY MEANS OF INDUCTIVE WALLS\*

V. K. NEIL and R. J. BRIGGS†

Lawrence Radiation Laboratory, University of California  
Livermore, California

(Received 1 December 1966)

**Abstract**—A method for suppressing the negative-mass instability in beams of particles with non-relativistic velocity is proposed and investigated theoretically. The method involves surrounding the beam with an inductive wall structure incorporating lumped-circuit inductors and does not rely on a velocity spread in the beam. The condition for stability of longitudinal oscillations of a given wavelength is  $v > v_p$ , where  $v$  is the particle velocity and  $v_p$  is the phase velocity of a wave with the same wavelength in the same structure, but with the beam replaced by a perfect conductor. A somewhat different structure consisting of a conducting ribbon wound in a helix around the beam is also analysed semi-quantitatively and shown to be effective in suppressing the instability.

## 1. INTRODUCTION

A METHOD of suppressing the negative-mass instability (NIELSEN, SESSLER and SYMON, 1959) in a beam of particles with relativistic velocity has been described in a previous work (BRIGGS and NEIL, 1966). The method does not rely on velocity spread in the beam to suppress the unstable longitudinal oscillations. By means of an inductive wall surrounding the beam, the electric-field configuration arising from the oscillations is altered in such a way that the oscillations become stable. Although the geometry and detailed analysis in the previous report apply mainly to beams in particle accelerators, the general principle is applicable to other geometries and to non-relativistic particle velocities. The purpose of this work is to extend the theory given in the earlier report to include the more complex wall structures necessary to stabilize non-relativistic and moderately relativistic beams.

This work was originally stimulated by the dramatic stabilization of the ion beam in a Calutron (SHIPLEY *et al.*, 1964) by placing various passive circuits in close proximity to the beam. However, it is not clear that the results of this work give any insight into the stabilizing mechanism in the Calutron. Indeed, the exact type of instability that was suppressed in the Calutron has not been identified. The experimental situation is complicated by the presence of cold plasma, which may play an important role in the instability and its suppression.

The necessary condition that longitudinal oscillations be stable may be stated in terms of the time-average energy of the perturbed electromagnetic field. The total magnetic energy must exceed the total electric energy in the region outside the beam. For oscillations in a relativistic beam enclosed by conducting walls, the two energies are nearly equal, but the magnetic energy is less than the electric energy. Therefore, only slight modifications of the wall are necessary to reverse this situation. In contrast, for non-relativistic particles the magnetic energy arising from the perturbation is very

\* Work performed under the auspices of the U.S. Atomic Energy Commission.

† Department of Electrical Engineering and The Research Laboratory of Electronics, Massachusetts Institute of Technology, Cambridge, Massachusetts.

frequency) in such machines will be at relatively low frequency, in the MHz range. At low frequencies the vacuum chamber impedance seen by the beam will be predominantly inductive. The wall image of the beam current will generate an effective voltage in the ring inductance which is again proportional to the slope of the line charge distribution (or, effectively, to the time derivative of the beam current). Below transition the phase of the beam induced voltage (with respect to the phase of the Fourier component of beam current which is generating it) is such that it will induce self bunching of the beam. This implies that the vacuum chamber induced voltage which is induced by a beam Fourier component resulting from externally applied rf voltage, will add to that voltage. The net effective voltage per turn seen by a particle within the bunch resulting from ring (inductive) impedance and the space charge self-voltage is expressed:

$$V_s = \frac{\partial \lambda(s)}{\partial s} \left[ \frac{g_o Z_o}{2\beta \gamma^2} - \Omega_o L \right] e\beta c \bar{R},$$

or

(1)

$$V_s = 2I_{dc} \frac{d}{dt} \sum_{m=1}^{\infty} F_n(m\omega_f) \cos(m\omega_f t) \left[ \frac{g_o Z_o}{2\beta \gamma^2 \Omega_o} - L(\omega) \right].$$

Questionable. !!



In these expressions  $[g_o = 1 + 2\ln(b/a)]$  where b and a are the nominal vacuum chamber aperture and beam radii<sup>(3)</sup>.  $Z_o = 377$  Ohms, and  $\Omega_o L$  is the vacuum chamber inductive reactance at the rotation frequency (nominally 15 -25 Ohms and referred to as  $Z/n$ ). The signs in the equations are consistent with the sign of the applied rf voltage below transition. In the second expression  $L(\omega)$  is meant to imply that the vacuum chamber inductance may be a function of frequency (i.e. part of the inductance may be due to presence of ferrite etc.).

The constant  $g_o$  may range from 2 to ~3 for the machines under consideration. The space charge term in the (first) expression above may fall in the range 100 - 250 Ohms. It appears reasonable to conclude that, at some chosen energy, the space charge effect may be cancelled exactly by intentionally increasing the ring inductive reactance and forcing the term in brackets to a very small value, or zero. This concept was proposed in 1968 by Sessler and Vaccaro<sup>(4)</sup> and later by R.K. Cooper et al<sup>(5)</sup> and by T Hardek<sup>(6)</sup> (1982).

[In 1966 V.K. Neil and R.J. Briggs proposed intentional insertion of inductance into particle beam vacuum chambers<sup>(7,8)</sup>, but this was intended as a proposal to stabilize ion beams against negative-mass instability. These proposals were presumably directed at situations where the beams were above transition, where introduction of inductance would have a stabilizing effect. In the proposal considered here, the opposite is true.]

EFFECTS OF SPACE CHARGE AND REACTIVE WALL IMPEDANCE  
ON BUNCHED BEAMS

S. Hansen, H.G. Hereward, A. Hofmann, K. Hübner, S. Myers

CERN  
Geneva, Switzerland

Space charge and reactive wall impedance create longitudinal forces inside the bunch which change the incoherent phase oscillation frequency, the bunch length and the size of the RF-bucket. These effects have been investigated with bunched beams in the ISR. By measuring the shift of the quadrupole mode phase oscillation frequency, the strength of the self-forces was determined. The inductive wall is dominant and its impedance (divided by the mode number) was measured to be  $|Z|/n = 26$  Ohms. An increase of bunch length with current was measured. It can be explained by the inductive impedance up to a certain current; beyond that an excessive, unexplained bunch lengthening occurs. The reduction of the bucket size affects the stacking process. By correcting for it, an increased density of the stacked beam was achieved.

## 1. Introduction

The longitudinal forces on a beam depend on its surroundings. The space charge forces of a beam in a perfectly conducting chamber have been calculated by Nielsen et al.<sup>1)</sup> A resistive surrounding can lead to the resistive wall instability, as shown by Neil and Sessler<sup>2)</sup>. An elegant method to deal with an inductive wall has been developed by Neil and Briggs<sup>3)</sup>; we will use it here. The effect of a general wall impedance has been treated by Sessler and Vaccaro<sup>4)</sup>.

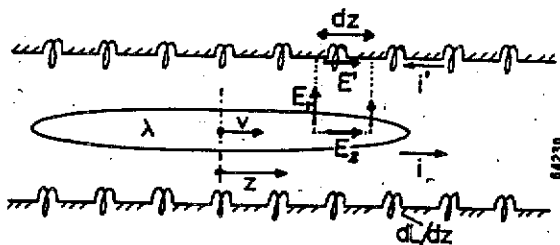


Fig. 1. Fields with inductive wall

We consider a bunch with a charge per unit length  $\lambda$  moving with velocity  $v = \beta c$  in a circular pipe as shown in fig. 1. The wall is considered to be perfectly conducting but has a distributed inductance  $dL/dz$  per unit length. We assume circular symmetry in the transverse directions and a line density  $\lambda$  which does not change much over a longitudinal distance of order of the chamber radius. The line charge produces a radial electric field  $E_r$  which is proportional to  $\lambda$ . The surface charges induced by this field on the chamber produce a wall current  $i'$  which has the same magnitude but opposite sign as the ac-component of the local beam current  $i$ . This current  $i'$  gives an electric field  $E'$  in the distributed wall inductance<sup>3)</sup>

$$E' = + \frac{dL}{dz} \frac{\partial i'}{\partial t} = - \frac{dL}{dz} \frac{\partial i}{\partial t} = - \frac{dL}{dz} e \beta^2 c^2 \frac{\partial \lambda}{\partial z}$$

By calculating the line integral  $\oint \vec{E} \cdot d\vec{s}$  along the dotted path indicated in fig. 1: the longitudinal field  $E_z$  in the beam is obtained

$$E_z = -e \frac{\partial \lambda}{\partial z} \left[ \frac{g_0}{4\pi \epsilon_0 \gamma^2} - \frac{dL}{dz} \beta^2 c^2 \right] \quad (1)$$

where  $g_0$  is the well known coupling coefficient. For a circular beam of radius  $a$  in a circular pipe of radius  $b$  this coefficient is  $g_0 = 1 + 2 \ln(b/a)$ . In the general case, where there is no circular symmetry, the situation is more complicated, but the properties of the wall can always be described by a coupling coefficient  $g_0$  and an inductance per unit length  $dL/dz$  which is seen by the beam.

Integrating the longitudinal field  $E_z(1)$  over the circumference  $2\pi R$  of the machine gives the voltage  $U_z$  per turn, seen by a particle which is at a distance  $z$  from the bunch centre

$$U_z = -e \frac{\partial \lambda(z)}{\partial z} \left[ \frac{R g_0}{2\epsilon_0 \gamma^2} - L \beta^2 c^2 \right] \quad (2)$$

where  $L$  is the total inductance per turn.

We assume now bunches with a parabolic line density distribution

$$\lambda(z) = \frac{6N}{l^3} \left[ \frac{l^2}{4} - z^2 \right], \quad \frac{\partial \lambda}{\partial z} = -\frac{12N}{l^3} z$$

with  $l$  = full bunch length,  $N$  = number of particles per bunch. This parabolic distribution is a very good approximation for the proton bunches in the ISR and produces self-fields which are linear in  $z$ . Using the total beam current  $I = e N f_0$  ( $M$  = number of bunches,  $f_0$  = rev. frequency) and replacing the total inductance  $L$  by its impedance  $|Z| = \omega L$  divided by the mode number  $n = \omega/2\pi f_0$

$$\left| \frac{Z}{n} \right| = 2\pi f_0 L$$

gives for the voltage per turn

$$U_z = \frac{3I}{\pi^2 M R} \left( \frac{2\pi R}{l} \right)^3 \left[ \frac{g_0 Z_0}{2\beta \gamma^2} - \left| \frac{Z}{n} \right| \right] z, \quad (Z_0 = \sqrt{\mu_0/\epsilon_0} = 377 \text{ Ohms}).$$

The external RF-voltage

$$U_{RF} = U_0 \sin \phi = U_0 ((\phi - \phi_s) \cos \phi_s + \sin \phi_s) = -U_0 \cos \phi_s \frac{h}{R} z + U_0 \sin \phi_s$$

( $h$  = harmonic number,  $\phi_s$  = synchronous phase angle) has to be added to  $U_z$ . The total voltage is

$$U = -U_0 \frac{h}{R} \cos \phi_s \left( 1 - \frac{3I}{\pi^2 h M U_0 \cos \phi_s} \left( \frac{2\pi R}{l} \right)^3 \left[ \frac{g_0 Z_0}{2\beta \gamma^2} - \left| \frac{Z}{n} \right| \right] z \right) + U_0 \sin \phi_s \quad (3)$$

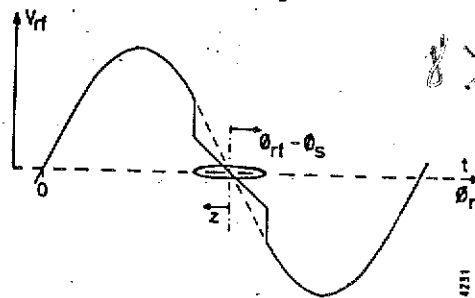


Fig. 2. RF-voltage with inductive wall

$\pi^2/4$  for  $q^2\pi^2$  small, vanishes for  $q^2\pi^2 \sim 6$ , attains a maximum value of approximately 4.5 for  $q^2\pi^2 \sim 20$ , and decreases thereafter. Finally, for the first Dirichlet solution, the

quantity  $[Z(0)]/\int_{-1}^1 Z^2 dx$  drops steadily from a unity for  $q^2\pi^2$  small, to 0.79 for  $q^2\pi^2 \sim 4$ , 0.37 at  $q^2\pi^2$  and 0.10 at  $q^2\pi^2 \sim 20$ .

## Coherent Electromagnetic Effects in High Current Particle Accelerators: III. Electromagnetic Coupling Instabilities in a Coasting Beam\*

L. JACKSON LASLETT†

Ames Laboratory, Iowa State University, Ames, Iowa, and Midwestern Universities Research Association, Madison, Wisconsin

AND

V. KELVIN NEIL AND ANDREW M. SEASLER‡

Lawrence Radiation Laboratory, University of California, Berkeley, California

(Received October 13, 1960)

The electromagnetic interaction of an intense relativistic coasting beam with itself, including the effect of a nonperfectly conducting vacuum tank, or a quiescent rf cavity, is investigated theoretically. It is shown that the resonances that may occur between harmonics of the particle circulation frequencies and the electromagnetic modes of the cavities can lead to a longitudinal instability of the beam. A criterion for stability of the beam against such longitudinal bunching is obtained as a restriction on the shunt impedance of the rf cavity, or the  $Q$  of the vacuum tank. This criterion contains the energy spread and intensity of the coasting beam, as well as the parameters of the accelerator. Numerical examples are given which indicate that, in general, the resonances with the vacuum tank will not cause instabilities, while those with an rf cavity can be prevented from causing instabilities by choosing the shunt impedance at a sufficiently low but still convenient value.

### I. INTRODUCTION

IN the second article (Part II) of this series<sup>1</sup> it was shown that a resonance can occur between a beam of particles in an accelerator and the characteristic electromagnetic modes of the vacuum tank. It is possible that this resonance could lead to instabilities in an intense relativistic coasting beam. This problem is distinguished from the longitudinal instabilities investigated previously by a number of authors<sup>2,3</sup> because resonance can occur

only with modes characterized by short wavenumbers in the azimuthal direction. Thus we shall be dealing with perturbation frequencies that are very high harmonics of the particle circulation frequency.

We shall again take a toroid with rectangular section as a model of the vacuum tank (Fig. 1), as all windows, discontinuities, and straight sections. Conductivity of the walls is sufficiently high so that vanishing of the tangential electric field to be a boundary condition in the solution of Maxwell's equations. Therefore, we can use the results in Part II of this series.

The stability of the coasting beam may also be affected by the presence of an rf cavity through which it must pass. If the cavity has an eigenfrequency harmonic of the beam circulation frequency, a resonance exists between the beam and the cavity. A resonance generally occurs for a much lower frequency than the resonance with the modes of the vacuum tank. For purposes of this calculation we assume that the beam is not driven externally.

Transverse particle motion will be neglected throughout this work, except insofar as it contributes to the sectional area of the beam. The density of the unperturbed beam is taken as being uniformly distributed. In Sec. II we assume an infinitesimal perturbation that preserves the cross-sectional dimensions of the



FIG. 1. Cutaway view of toroidal cavity.

\* This work was done under the auspices of the U. S. Atomic Energy Commission.

† Now in London with the Office of Naval Research.

‡ Permanent address: Ohio State University, Columbus, Ohio.

<sup>1</sup> V. K. Neil, D. L. Judd, and L. J. Laslett, *Rev. Sci. Instr.* 32, 267 (1961).

<sup>2</sup> A. A. Kolomenaky and A. N. Lebedev, *Proceedings of the CERN Symposium on High Energy Accelerators, Geneva 1959* (CERN, Geneva, 1959), p. 115.

<sup>3</sup> C. E. Nielsen, A. M. Seasler, and K. R. Symon, *Proceedings of the CERN Symposium on High Energy Accelerators, Geneva, 1959* (CERN, Geneva, 1959), p. 239.

ON INTENSITY LIMITATIONS IMPOSED BY TRANSVERSE SPACE-CHARGE EFFECTS  
IN CIRCULAR PARTICLE ACCELERATORS

L. J. Laslett  
Lawrence Radiation Laboratory

Contents

I. Introduction .....	325
II. Transverse Space-Charge Effects -- Axial Stability Limit	
A. Single-Particle Stability	
1. The Assumed Fields .....	327
2. The Equation of Motion .....	330
3. The Image-Force Coefficients .....	332
a. The electrostatic image coefficient, $\epsilon_1$	
(1) Plane-parallel conducting surfaces .....	333
(2) Elliptical boundary .....	333
b. The magnetostatic image coefficient, $\epsilon_2$	
(1) Plane-parallel magnet poles .....	335
(2) Wedge-shaped magnet gap .....	337
(3) Other pole configurations .....	339
B. Stability with Respect to a Collective Transverse Displacement	
1. The Assumed Fields .....	341
2. The Equation of Motion .....	341
3. The Image-Force Coefficients .....	343
a. The electrostatic image coefficient, $\xi_1$	
(1) Plane-parallel conducting surfaces .....	343
(2) Elliptical boundary .....	343
b. The magnetostatic image coefficient, $\xi_2$	
(1) Plane-parallel magnet poles .....	345
(2) Wedge-shaped magnet gap .....	345
III. Examples .....	347
Appendix A -- Application of Conformal Transformations .....	350
Appendix B -- Images in Infinite Parallel Conducting Planes	
1. Application of Conformal Transformation .....	352
2. Direct Summation of Image Fields .....	353
Appendix C -- Images in Infinite Plane-Parallel Ferromagnetic Poles	
1. Application of Conformal Transformation .....	355
2. Direct Summation of Image Fields .....	356
Appendix D -- Electrostatic Images in an Elliptical Conducting Cylinder ...	357
Appendix E -- Magnetic Images for a Wedge-Shaped Gap .....	363

## CONCLUSIONS

- Insertion of inductance for passive compensation of longitudinal space charge potential well distortion works as advertised (below transition).
- In some cases over-compensation may be useful. It may provide beam induced focusing not easily generated by external rf voltage.
- It is inexpensive, with very low operating cost.

But problems associated with the real part of the permeability; may cause instabilities  
and could cause undesired increase in bunching factor or increased Laslett tune shift.